Iris Boundary Detection Using An Ellipse Integro Differential Method

Mahboubeh Shamsi
Faculty of Electrical and Computer Engineering
University of Technology, Qom, Iran
shamsi@qut.ac.ir

Abdolreza Rasouli Kenari
Faculty of Electrical and Computer Engineering
University of Technology, Qom, Iran
rasouli@qut.ac.ir

Abstract. Iris segmentation is the principal task of Iris based biometric identification systems. Always the low contrast between pupil and iris always affects on accuracy of detecting boundary between them. In order to increasing the accuracy of boundary detecting, we propose a new technique using a difference function and a factor matrix. We also enhance the technique to detect the pupil and iris as ellipse instead of circle. Experiments show that the proposed technique can segment the iris region and pupil region precisely. Based on our result, 99.34% of eyes have been segmented accurately in 1.24s averagely.

Keywords. Daugman's method, Average Square Shrinking, Difference Function, Contour Factor Matrix

I. INTRODUCTION

Iris is the most reliable biometric in secure transaction proposals. Iris in an eye image is situated between sclera and pupil. Before iris can be utilized for a specific application, it has to be localized first. Iris localization is a challenging ordeal due to several reasons such as occlusions to the presence of eyelids and eyebrows and also due to the uneven texture contrast [1-2]. The textural contrast between sclera and iris is high; conversely the textural contrast between iris and pupil is low [3-5]. The problem is further aggravated with the presence of light reflection in the pupil. Hence, an accurate algorithm is desired to detect the subtle difference between the two regions. In this paper, we propose a new algorithm to capture a maximum difference value of both, inner and outer iris boundaries.

This paper next describes related work, followed by new algorithm in section III. The paper then continues on result in section IV. The paper ends with a conclusion in section V.

II. RELATED WORK

Iris is between sclera and pupil. Sclera region and iris region is easier to differentiate due to higher texture contour contrast between the two regions. However, there is a lower texture contrast between iris region and pupil region. Hence, it is difficult to automatically detect the edge between iris and pupil [6].

Daugman [6] uses a differential operator for locating the circular iris, pupil regions and the arcs of the upper and lower eyelids. The differential operator is defined as

$$\max_{(r,x_0,y_0)}\left|G_\delta(r)*\frac{\partial}{\partial_r}\oint_{r,x_0,y_0}\frac{I(x,y)}{2\pi r}d_s\right| \tag{1}$$

Where $I(x, y)$ is the gray level of image in pixel (x, y), $G_{\delta(r)}$ is Gaussian smoothing filter, s is the counter of circle represented by (x_0, y_0) as center and r as radius. The operator searches for the circular path where there is maximum change in pixel values, by varying the radius and centre x and y position of the circular contour. However, if there is noise in the image, the algorithm can fail, such as reflection. When the iris is dark and the image is under natural light, the contrast between iris and pupil is low and it makes the segmentation process more difficult [7].

An automatic segmentation algorithm based on the circular Hough transform is employed by Wildes *et al*. [8-9]. They also make use of the parabolic Hough transform to detect the eyelids, approximating the upper and lower eyelids with parabolic arcs, which are represented as;

$$\begin{aligned}&\left(-\left(x-h_j\right)\sin\theta_j+\left(y-k_j\right)\cos\theta_j\right)^2=\\&a_j\left(\left(x-h_j\right)\cos\theta_j+\left(y-k_j\right)\sin\theta_j\right)\end{aligned} \tag{2}$$

Where a_j is the controls of the curvature, (h_j, k_j) is the peak of the parabola and θ_j is the angle of rotation relative to the x axis. For edge detection in this method we need to choose threshold values.

Camus and Wildes [8] use similar method to Daugman's method [10]. Their algorithm, finds three circumference parameters (centre (x, y) and radius z) by maximizing the following function

$$C=\sum_{\theta=1}^{n}\left((n-1)\left\|g_{\theta,r}\right\|-\sum_{\phi=\theta+1}^{n}\left\|g_{\theta,r}-g_{\phi,r}\right\|-\frac{I_{\theta,r}}{n}\right) \tag{3}$$

Where n is the total number of directions and $I_{\theta,r}$ and $g_{\theta,r}$ are the image intensity and derivatives with respect to the radius in the polar coordinate system respectively.

The performance of algorithm degraded for noisy iris images and when there is reflection in the image.

Daugman's operator is based on the fact that the illumination difference between inside and outside of pixels in iris edge circle is maximum [11]. It means the difference values of pixel's gray level in iris circle are higher than any other circles in image. This fact is based on color of iris and color of sclera.

We are not able to calculate Daugman Operator for all feasible circles of an image. Therefore, we should restrict the space of potential circles. Many researchers assume that the center of iris is near the center of image. But in many cases, the center of iris does not fit to the center of image. Also they find a range of radius which is based on the size of image.

In our first paper, we proposed a new Average Square Shrinking (ASS) Approach [12] for initializing the range of potential centers. Therefore, we restricted the algorithm to a range of (x, y) as potential centers and a range of r as potential radiuses. The ASS approach is based on this fact that all eyes' pupils are black and therefore the center of iris must be black. Gaussian Blur or other smoothing method is applied to find dark integrated pixels in image processing methods. Therefore we used the darkest place to detect the center of the iris. We had broken the image to some small squares. Each square in a source image will be converted into one pixel in shrunken image during ASS process. The size of square and the stages of shrinking are related to shrinking (smoothing) factor S_f and number of shrinking stages N respectively. The values of all pixels inside the square will be averaged in the shrunken image. The darkest pixel (x_0, y_0) in the last image is the pupil center. The range of $[x_0 \pm S_f] \times [y0 \pm S_f]$ will be used for potential centers of Daugman operator.

We had converted the Daugman's environmental integral to a discreet summation of a simple difference function on circle's contour to be computable by computer programming. The difference function is

$$diff(x,y) = I(x+\Delta_\alpha, y+\Delta_\alpha) - I(x-\Delta_\alpha, y-\Delta_\alpha) \qquad (4)$$

We showed that the difference function also should be computed approximately, because we had only integer values for coordinates (x, y) and we could not calculate exact difference values. We had only the values of top, bottom, left, right and diagonal pixels. Due to this, we converted the Daugman operator as follows:

$$\begin{aligned}
&\max_{(x_c,y_c,r)} \sum_{j=1}^{CS} diff(x_j,y_j) \;\; \forall (x_c,y_c) \in potential\ centers \,\&\, r \in potential\ radius \\
&x_j = x_c + r\cdot\cos(\alpha_j), y_j = y_c + r\cdot\sin(\alpha_j), \alpha_j = 2\pi * {}^{j}\!/_{CS} \\
&diff(x_j,y_j) = I_1 + I_2 + I_3 + I_4 \\
&I_1 = \left(I(x_j+1,y) - I(x_j-1,y)\right)\cdot\cos(\alpha_j), I_2 = \left(I(x,y_j+1) - I(x,y_j-1)\right)\cdot\sin(\alpha_j) \\
&I_3 = \left(I(x_j+1,y_j+1) - I(x_j-1,y_j-1)\right)\cdot\sin(45+\alpha_j) \\
&I_4 = \left(I(x_j+1,y_j-1) - I(x_j-1,y_j+1)\right)\cdot\cos(45+\alpha_j)
\end{aligned} \qquad (5)$$

However, our previous method worked very well, but it did not compute the difference value correctly. The performance of our algorithm degraded for low texture contrast eye's image.

III. Proposed Algorithm

We use the Average Square Shrinking Process to find the potential centers and the estimated range of radius. Then, we apply the Daugman operator for improving the iris center and radius. The higher value of Daugman operator corresponded to the exact center and radius of iris. These steps will be continued iteratively on higher shrunk image to find the final center and radius.

A. Ellipse Segmentation

The experiment was conducted on many eyes' images; it has been observed that so many irises are not exactly circle. So an ellipse view will improve the accuracy of iris segmentation. We have made a slight modification to Daugman's operator to make it desirable for ellipse function. The new operator is:

$$\max_{(r_a,r_b,x_0,y_0)} \left| G_\delta(r) * \frac{\partial}{\partial_r} \oint_{r_a,r_b,x_0,y_0} \frac{I(x,y)}{2\pi\sqrt{\frac{1}{2}\left(r_a^2+r_b^2\right)}} d_s \right| \qquad (6)$$

Two parameters r_a, r_b have been replaced by radius parameter r. The new operator is able to look for any feasible ellipse around the iris to find the best match.

B. Improving Difference function

The Daugman Operator tries to compute the difference gray level value between inside and outside pixels of iris circle. Daugman demonstrated that this value is the greatest one between all feasible circles of an eye image [13].

There are discrepancies in the difference function created in our first algorithm as described next. The difference function computes the difference value by subtracting the opposite pixels. These opposite pixels are right and left pixels, top and bottom and two pair of diagonal pixels. Fig 1.1.a shows the problem of this assumption that should be removed. The outside and inside pixels of difference

function are colored in Fig 1.a. The gray rectangles are outside pixels set and hatched rectangles are inside pixels. Let us highlight the problem by an example. If you focus on $Octad_5$, the gray rectangles are really inside the circle, whereas they are assumed as outside pixels in difference function.

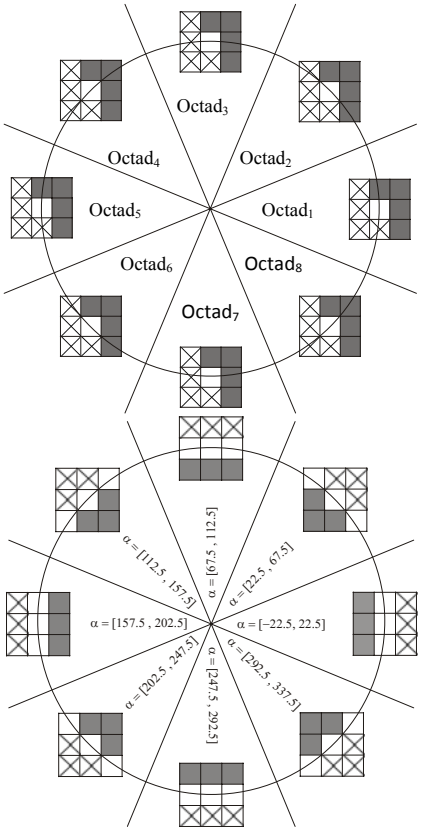

Figure 1. a)The Wrong Pixel Setting. b) Correct Pixel Setting

The correct adjustment of outside and inside pixels around the circle's contour is shown in Fig 1.b.

We have only eight pixels around the main pixel. So we divide the circle to eight regions, because the outside and inside states of pixel in each region are the same. This fact is shown in Fig 1.b. Each region covers $2\pi/8$ or $\pi/4$ which is equal to 45°. First the center degree of each region is computed, because each region corresponds to its center. The center of each region is represented as θ_j with 22.5° offset as follows:

$$\theta_j = \left(\left\lfloor \frac{\alpha_j + 22.5}{45} \right\rfloor \times 45 \right) \tag{7}$$

We proposed a new factor matrix with 3×3 dimension. The matrix is multiplied by the neighbors of the main pixel correspondingly. The factor matrix values are selected from (-1, 0, 1). The multiplication factors for outside pixel is 1 and for contour and inside pixels are 0 and -1, respectively. By adding the values of pixels after applying the factors, we obtain the real difference between outside and inside pixels. The factor matrix is:

$$M = \begin{bmatrix} \sin\left((\theta_j - 45)\times\left(\frac{2\pi}{360}\right)\right) & \sin\left((\theta_j)\times\left(\frac{2\pi}{360}\right)\right) & \sin\left((\theta_j + 45)\times\left(\frac{2\pi}{360}\right)\right) \\ \sin\left((\theta_j - 90)\times\left(\frac{2\pi}{360}\right)\right) & 0 & \sin\left((\theta_j + 90)\times\left(\frac{2\pi}{360}\right)\right) \\ \sin\left((\theta_j - 135)\times\left(\frac{2\pi}{360}\right)\right) & \sin\left((-\theta_j)\times\left(\frac{2\pi}{360}\right)\right) & \sin\left((\theta_j + 135)\times\left(\frac{2\pi}{360}\right)\right) \end{bmatrix} \tag{8}$$

Some examples of factor matrix are shown below.

$$\alpha = [-22.5, 22.5] \Rightarrow M = \begin{bmatrix} -1 & 0 & 1 \\ -1 & 0 & 1 \\ -1 & 0 & 1 \end{bmatrix}$$

$$\alpha = [\ 22.5, 67.5] \Rightarrow M = \begin{bmatrix} 0 & 1 & 1 \\ -1 & 0 & 1 \\ -1 & -1 & 0 \end{bmatrix}$$

$$\alpha = [67.5, 112.5] \Rightarrow M = \begin{bmatrix} 1 & 1 & 1 \\ 0 & 0 & 0 \\ -1 & -1 & -1 \end{bmatrix}$$

The factor matrix ensures the correct setting for outside and inside pixels as shown in Fig 1.b. So the new difference function, diff(x, y) is:

$$\max_{(x_c, y_c, r_a, r_b)} \sum_{j=1}^{CS} diff(x_j, y_j) \ \forall (x_c, y_c) \in potential\ centers \,\&\, r_a, r_b \in potential\ radius$$

$$x_j = x_c + r_a \cdot \cos(\alpha_j), y_j = y_c + r_b \cdot \sin(\alpha_j), \alpha_j = 360 * {}^{j}\!/_{CS}, \theta_j = \left(\left\lfloor \frac{\alpha_j + 22.5}{45} \right\rfloor \times 45 \right) \tag{9}$$

$$diff(x_j, y_j) = \left| \sum_{\tilde{i}=1}^{3} \sum_{\tilde{j}=1}^{3} \tilde{I}_{\tilde{i},\tilde{j}} \right|, \tilde{I} = M \circ \begin{bmatrix} I(x_j - 1, y_j - 1) & I(x_j, y_j - 1) & I(x_j + 1, y_j - 1) \\ I(x_j - 1, y_j) & I(x_j, y_j) & I(x_j + 1, y_j) \\ I(x_j - 1, y_j + 1) & I(x_j, y_j + 1) & I(x_j + 1, y_j + 1) \end{bmatrix}$$

We delete the number of stages parameter *N* that is required to be input manually. This is accomplished by adopting a threshold for the size of the last shrunken image. The image is shrunk until the size of image is less than the

threshold. Consequently, the range of radius parameter can also be ignored, since in an eye image with width 10 pixels, the radius can be estimated by 2 pixels.

IV. EXPERIMENTAL RESULT

The algorithm is developed using Delphi programming language. It is tested on 2.4 GHz CPU with Windows Vista and 2 GB Ram. Two famous iris databases have been selected for experiments. CASIA-IrisV3 [14] includes three subsets which are labeled as CASIA-IrisV3-Interval, CASIA-IrisV3-Lamp, CASIA-IrisV3-Twins. CASIA-IrisV3 contains a total of 22,051 iris images from more than 700 subjects. All iris images are 8 bit gray-level JPEG files, collected under near infrared illumination. MMU iris database [15] contributes a total number of 450 iris images. Subjects come from Asia, Middle East, Africa and Europe. Each of them contributes 5 iris images for each eye.

The maximum value of difference function for edge between sclera and iris (outer boundary) and for edge between iris and pupil (inner boundary), are computed using the previous algorithm and the current algorithm. The results are depicted in Fig 2, 3. In addition, we investigate the effect of circle sample (*CS*) on the maximum value of difference function. It is noticed that, as the circle sample increases, so does the maximum value of difference function. Hence, the circle sample is relatively proportional to maximum value of difference function. The results show that with the low value of CS both algorithms display a similar performance and there is no significant variation between difference values. However, by increasing CS, the distinction of difference value on the new algorithm will be extremely improved. The amount of circle contour sample (CS) versus detection accuracy and time consuming has been studied in [12, 16]. With choosing correct amount of CS, the manual inference of user decreases.

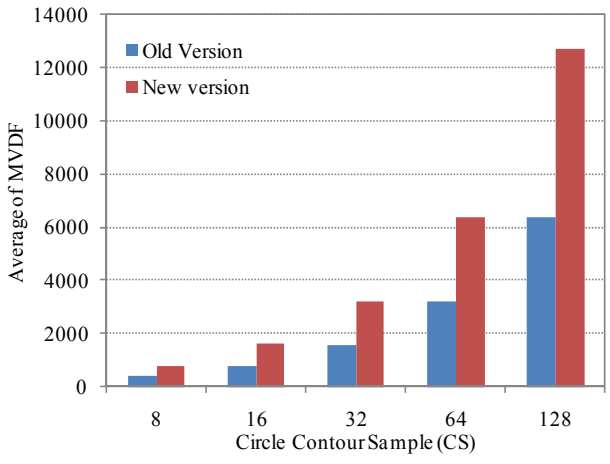

Figure 2. Maximum Value Related to CS for Iris Circle

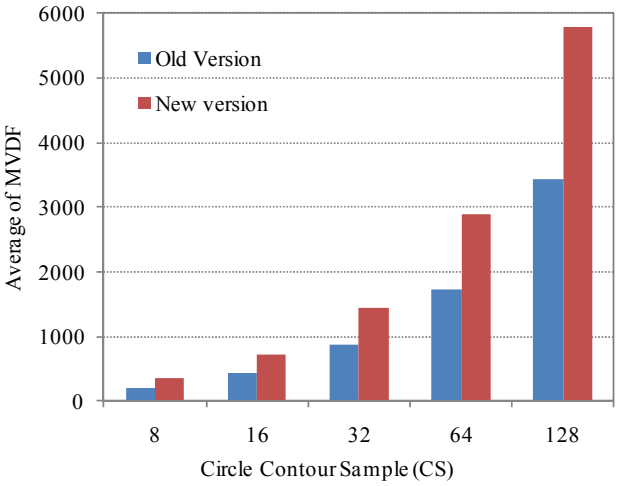

Figure 3. Maximum Value Related to CS for Pupil Circle

It is noticed that the maximum difference value is doubly increased in the new algorithm for both outer and inner iris boundaries when compared to our previous algorithm. The maximum difference value is bigger for outer boundaries as compared to inner boundaries. This is due to the high texture contrast between sclera and iris. Conversely, the small difference value for inner boundary is due to the low texture contrast between iris and pupil.

The result of ellipse operator has been shown in Fig 4. It is disclosed that the ellipse operator redounded to better segmentation and accuracy has been extremely increased. But, due to increasing one more radius parameter, we expect that the processing time increases, respectively. So we compare the performance and processing time of our new algorithm with other algorithms obtained from [17]. Table 1 shows the boundary detection rate of various algorithms in comparison to our algorithm.

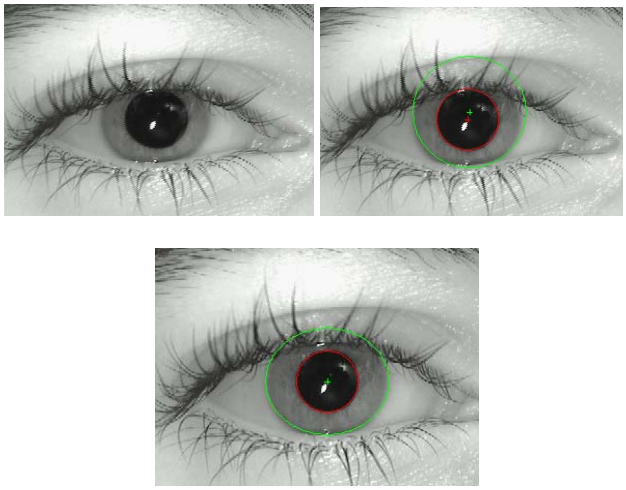

Figure 4. The Original image and result of Ellipse operator vs. Circle operator

TABLE I. DETECTION RATE OF PROPOSED ALGORITHMS

Algorithm	Time (s)	Detect Rate
Daugman [18]	5.36	98.58%
Daugman [19]	0.984	54.44%
Wildes [18]	6.34	99.82%
Wildes [19]	1.35	86.49%
Masek [19]	7.5	83.92%
Proposed Algorithm	1.24	99.34%

With regards to Table 1, it is noticed that our new algorithm shows the highest rate of iris boundaries detection related to its execution time in comparison to existing algorithms. Based on these findings, we are confident that the subsequent step of feature extraction will aid us to produce good quality textural features for further analysis.

V. CONCLUSION

The detection of iris boundaries is a difficult task in iris recognition systems. This is due to the low texture contrast between pupil region and iris region. In this paper, we hybrid summation function and factor matrix to be able to detect the iris boundaries. Both theoretically and our experimental results show that the proposed new algorithm strongly improved the Daugman Operator Difference Function and the detection accuracy has been significantly improved by new algorithm. The segmentation rate using this algorithm is 99.34%.

REFERENCES

[1] J. h. Park, et al., "Iris Tilt Correctness in Iris Recognition System," WSEAS Trans. Info. Sci. and App., vol. 1, pp. 139-144, 2004.

[2] C. T. Yuen, et al., "Real-Time Detection of Face and Iris," WSEAS TRANSACTIONS on SIGNAL PROCESSING, vol. 5, pp. 209-218, 2009.

[3] W. Fenghua, et al., "Iris recognition based on multialgorithmic fusion," WSEAS Trans. Info. Sci. and App., vol. 4, pp. 1415-1421, 2007.

[4] H. E. Kocer and N. Allahverdi, "An efficient iris recognition system based on modular neural networks," presented at the Proceedings of the 9th WSEAS International Conference on Neural Networks, Sofia, Bulgaria, 2008.

[5] G. S. El-taweel and A. K. Helmy, "Efficient iris recognition scheme based on difference of filters," WSEAS Trans. Comp. Res., vol. 3, pp. 152-161, 2008.

[6] J. Mazur, "Fast Algorithm for Iris Detection," Advances in Biometrics, vol. 4642, pp. 858-867, 2007.

[7] J. G. Daugman, "How iris recognition works," Proceedings of 2002 International Conference on Image Processing, 2002.

[8] T. A. Camus and R. Wildes, "Reliable and fast eye finding in closeup images," IEEE 16th Int. Conf. on Pattern Recognition, Quebec, Canada, pp. 389-394, 2004.

[9] R. Wildes, et al., "A system for automated iris recognition," Second IEEE Workshop on Applications of Computer Vision, pp. 121 - 128 2004.

[10] J. G. Daugman, et al., "Combining Crypto with Biometrics Effectively," IEEE Trans. on Computers, vol. 55, 2006.

[11] M. Shamsi, et al., "Iris Image Localization using Binning Approach," Proceedings of 2008 Student Conference on Research and Development (SCOReD 2008), 2008.

[12] M. Shamsi, et al., "Fast Algorithm for Iris Localization Using Daugman Circular Integro Differential Operator," International Conference of Soft Computing and Pattern Recognition, SoCPaR09, 2009.

[13] M. Shamsi, et al., "Iris Segmentation and Normalization Approach," Journal of Information Technology (Universiti Technologi Malaysia), vol. 19, 2008.

[14] CASIAIRISREP. CASIA iris image database [Online].

[15] MMUIRISREP. MMU iris image database, [Online].

[16] M. Shamsi, et al., "Iris Boundary Detection Using A Novel Algorithm," in The 9th WSEAS International Conference on Applications of Computer Engineering (ACE'10) - (ISI, Elsevier Indexed), Penang, Malaysia, 2010.

[17] H. Proenca and L. A. Alexandre, "Iris segmentation methodology for non-cooperative recognition," IEEE Proceedings on Vision, Image and Signal Processing, vol. 153, pp. 199-205, 2006.

[18] H. Nguyen Van and K. Hakil, "A Novel Circle Detection Method for Iris Segmentation," presented at the Proceedings of the 2008 Congress on Image and Signal Processing, Vol. 3 - Volume 03, 2008.

[19] S. P. Narote, et al., "An Automated Segmentation Method For Iris Recognition," in IEEE Region 10 Conference (TENCON 2006), 2006, pp. 1-4.